ELSEVIER

Journal of Alloys and Compounds 356–357 (2003) 738–741

Journal of ALLOYS AND COMPOUNDS

www.elsevier.com/locate/jallcom

Deterioration behavior of a multi-phase vanadium-based solid solution alloy electrode

N. Kuriyama[a,*], M. Tsukahara[b], K. Takahashi[b], H. Yoshinaga[c], H.T. Takeshita[a], T. Sakai[a]

[a] *AIST, 1-8-31 Midorigaoka, Ikeda-shi, Osaka 563-8577, Japan*
[b] *IMRA Material R&D Co. Ltd., Kariya-shi, Aichi 448-0021, Japan*
[c] *Taiyo Koko Co. Ltd., 1603-1 Higashioki, Nakahiro Ako-shi, Hyogo 678-0232, Japan*

Received 1 September 2002; accepted 19 December 2002

Abstract

Deterioration behavior of an electrode made of $V_4TiNi_{0.65}Co_{0.05}Nb_{0.047}Cr_{0.058}$ was studied by means of impedance spectroscopy, scanning electron microscopy (SEM) and impedance spectroscopy. The reaction resistance related to the lowest frequency semi-circle increased considerably and dischargeability became worse with cycling. The double layer capacitance for the same semi-circle became smaller after 50 cycles. The SEM observation of the cross-section of the cycled electrodes indicated that voids were formed around alloy particles embedded in a matrix of Cu powder, and crack formation and dissolution of the TiNi second phase proceeded with cycling. These phenomena indicate that dissolution of the second phase caused loss of reaction sites and TiNi networks as a current collector.

Keywords: Impedance spectroscopy; Deterioration; Metal hydride electrode; Multi-phase; V-based alloy

1. Introduction

Vanadium-based solid solution alloys, for example $V_3TiNi_{0.56}$, are known to have a large effective hydrogen capacity as a metal hydride electrode [1]. The alloys consist of two phases: a primary phase of a vanadium-based solid solution and a three-dimensional boundary phase of TiNi which acts as a micro-current collector. In spite of its high capacity, over 400 mA/g, the discharge capacity decreases more steeply with cycling than in the case of conventional AB_5 alloys for battery. In order to clarify the origin of the loss of discharge capacity, we studied deterioration behavior of an electrode made of $V_4TiNi_{0.65}Co_{0.05}Nb_{0.047}Cr_{0.058}$ by means of impedance spectroscopy and scanning electron microscopy (SEM).

2. Experimental

The alloy, $V_4TiNi_{0.65}Co_{0.05}Nb_{0.047}Cr_{0.058}$, was pulverized to under 150 μm by hydrogenation. A fine copper powder of average diameter ~2.3 μm was used for all electrodes. First 1 part by weight of the alloy powder and 3 parts of the copper powder were mixed in an agate and pressed into an electrode pellet (~1 g, 13 mm in diameter) at 7.5 ton/cm^2. The pellet was then sandwiched between a Ni mesh (100 mesh) with a Ni wire for electrical contact [2].

A 6 mol·dm^{-3} KOH aqueous solution, a sintered $Ni(OH)_2$/NiOOH electrode as a counter electrode, and a Hg/HgO electrode as a reference electrode were used in all experiments. Charge–discharge cycles for the electrodes were performed at 20 °C. The electrodes were charged at 100 mA/g for 5 h (500 mAh/g) for all cycles, and discharged at 40 and 100 mA/g (at 13th and 50th cycles). The discharge process after 30-min charge rest was terminated at −0.65 V (vs. Hg/HgO). Impedance spectra of the electrodes were measured at the depth of discharge, 10, 45, 80 and 100%, at the third, 13th and 50th cycles. Impedance spectra were recorded from 10 kHz to 0.5 mHz at the amplitude of perturbation to the electrodes, 5 mV_{P-P} under open-circuit condition [3].

The electrodes which were charged and discharged for three, 13 and 50 cycles were rinsed well with distilled water after being completely discharged, and epoxy resin

*Corresponding author.
E-mail address: kuriyama-n@aist.go.jp (N. Kuriyama).

0925-8388/03/$ – see front matter
doi:10.1016/S0925-8388(03)00163-4

was impregnated into the electrode pellet. The polished surface of the pellets in epoxy resin was observed with SEM.

3. Results and discussion

Nyquist plots of impedance spectra for the electrodes at the third, 13th and 50th cycles are shown in Fig. 1. Those Nyquist plots consist of three obvious semi-circles, A, B and C, as schematically illustrated in Fig. 2. This characteristic is different from spectra already reported for metal hydride electrodes, though contribution of a small semi-circle which corresponds to B should be included for complete fitting of the spectra in the previous results [2]. The equivalent circuit shown in Fig. 2 consists of R_i (i=1~4) indicating a resistive component and Q_i indicating a capacitive component of which impedance $Q_i(\omega)$ is expressed by a constant phase element: $Q_i(\omega) = Y_{0i}(j\omega)^{-\psi}$, where Y_{0i} corresponds to capacitance, ω is frequency, and ψ is a parameter between 0 and 1 [2]. $1/R_3$ and Y_{03} representing the semi-circle B in Fig. 2 and $1/R_4$ and Y_{04} representing C were proportional to amount of alloy, although $1/R_2$ and Y_{02} representing the semi-circle A were independent of amount of alloy. These facts show that the semi-circles B and C are related to processes at the surface of alloy particles. Based on the assignment in Ref. [2], the semi-circle B is assigned to contact resistance between alloy particles and Cu powder matrix of the electrode, and C is assigned to reaction resistance on alloy particles. Details of these assignments and behavior of impedance spectra of the electrode will be reported elsewhere. The semi-circle A is attributed to the resistance and capacitance between the alloy pellet and the current collector [3].

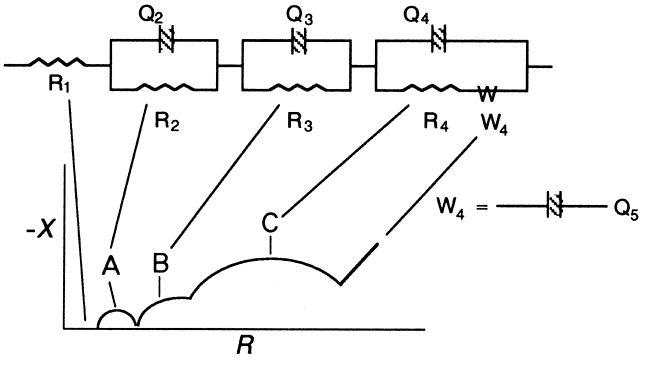

Fig. 2. Schematic Nyquist plot of the impedance spectra of the $V_4TiNi_{0.65}Co_{0.05}Nb_{0.047}Cr_{0.058}$ electrode with three semi-circles (A, B and C) and an equivalent circuit to analyze the Nyquist plots.

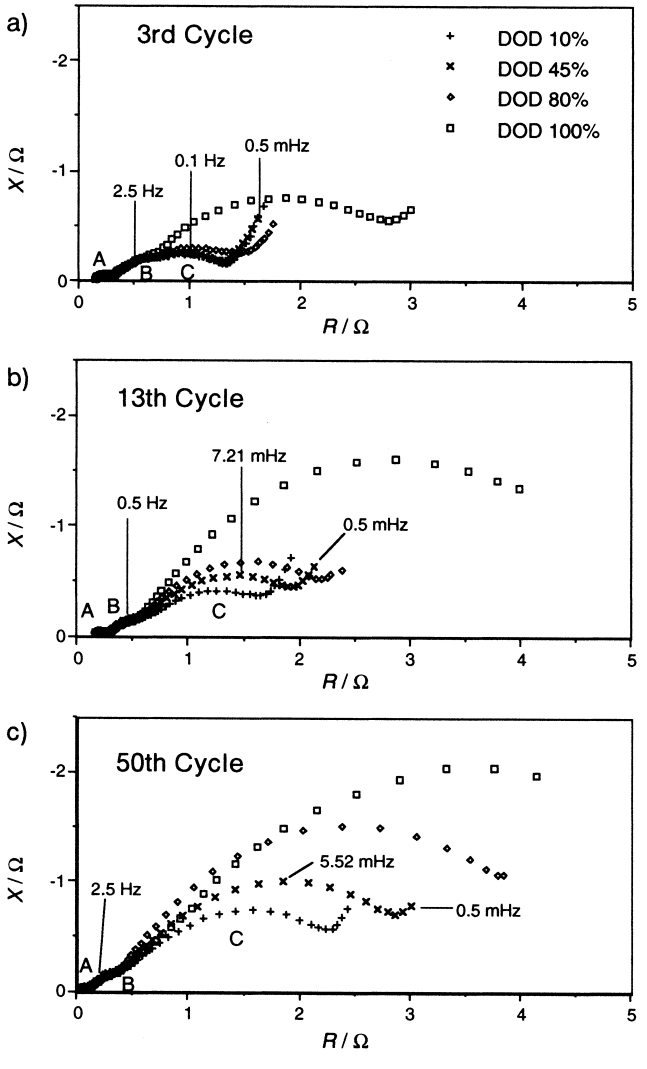

Fig. 1. Nyquist plots of the impedance spectra of the $V_4TiNi_{0.65}Co_{0.05}Nb_{0.047}Cr_{0.058}$ electrode at 20 °C at the third, 13th and 50th cycles. Three semi-circles, A, B and C, were clearly observed.

Parameters fitted to the Nyquist plots at depth of discharge (DOD) 45% of the electrode and discharge capacities are shown in Table 1. Time constant, $R_4 \cdot Y_{04}$, represents inverse of activity of alloy surface, because R_4 is inversely proportional to both surface area and activity of the electrode but Y_{04} is proportional to surface area. Parameters for a $Zr_{0.9}Ti_{0.1}Ni_{1.1}Co_{0.1}Mn_{0.6}V_{0.2}$ electrode are included in Table 1 as an example of Nyquist plots of typical metal hydride electrodes.

The electrode of the Ti–V–Ni-based multi-phase alloy indicated deterioration of dischargeability. While the decrease in discharge capacity at 40 mA/g was small, an appreciably large decrease at 100 mA/g was observed between the 13th and 50th cycles. This fact suggests that loss of activity of the electrode during cycling should be significant, though intrinsic capacity of the electrode was expected to decrease by ~20%.

The parameters of the equivalent circuit for the Ti–V–Ni-based multi-phase alloy show some large changes,

Table 1
Parameters of the equivalent circuit at DOD 45% shown in Fig. 2 and discharge capacity, *C*, of the Ti–V–Ni-based alloy and a Zr-based Laves alloy for comparison

Cycle	R_3/Ω	Y_{03}/F	R_4/Ω	Y_{04}/F	$R_4 \cdot Y_{04}$/s	*C* (40 mA/g) /mAhg^{-1}	*C* (100 mA/g) /mAhg^{-1}
$V_4TiNi_{0.65}Co_{0.05}Nb_{0.047}Cr_{0.058}$							
$n=3$	0.296	0.331	0.711	1.94	1.38	327	
$n=13$	0.387	0.846	1.45	6.78	9.83	369	348
$n=50$	0.368	1.02	2.80	4.94	13.8	308	181
$Zr_{0.9}Ti_{0.1}Ni_{1.1}Co_{0.1}Mn_{0.6}V_{0.2}$							
$n=30$	0.0997	0.251	0.655	0.432	0.283	–	–

especially in reaction resistance R_4 and double layer capacitance Y_{04} for the surface of the alloy particles. Considerable increase from the third to the 13th cycle in time constant, $R_4 \cdot Y_{04}$, which is inversely proportional to activity of the electrode, shows decrease in activity of the alloy surface. Large increase in Y_{04}, which is proportional to surface area of the electrode, between those cycles indicates enlargement of surface area of the electrode. Therefore increase in surface area of the electrode compensates for loss of activity. On the other hand, Y_{04} decreases by 27% between the 13th and the 50th cycles, and time constant, $R_4 \cdot Y_{04}$, increases by 40%. As a result, appreciable increase in R_4 is considered to decrease discharge capacity at higher current density.

Fig. 3 shows change of cross-sectional views of the electrode with cycling. At the third cycle, gaps between alloy particles and a Cu matrix were formed. At the 13th cycle, the gaps became wider, and cracks in the TiNi phase (light gray region with network structure) became obvious. Formation of gaps is expected to increase in contact resistance between alloy particles and a Cu matrix. In addition, larger region with gap results in higher capacitive component. This agrees with increase in R_3 and Y_{03} between the third and 13th cycles. Contribution from R_3 and Y_{03} is much smaller than that of R_4 and Y_{04}.

At the 50th cycle, consequently, most of the TiNi phase disappeared and the Ti–V main phase remained. Increase in Y_{04} between the third and 13th cycles and decrease in Y_{04} between the 13th and 50th cycles agree with formation of many cracks in the TiNi phase with activity for electrochemical reactions and disappearance of the TiNi phase, because Y_{04} is proportional to the reactive surface area. Considerably large Y_{04} with respect to that of the $Zr_{0.9}Ti_{0.1}Ni_{1.1}Co_{0.1}Mn_{0.6}V_{0.2}$ electrode in Table 1 shows contribution of the cracks in the TiNi phase to Y_{04}. In addition, since decrease in activity corresponding to increase in time constant, $R_4 \cdot Y_{04}$, was observed at the 13th and 50th cycles, the TiNi surface is considered to be easily deactivated after new surface in the cracks appeared because of dissolution of the electrochemically active TiNi phase.

According to the above considerations, the crack forma-

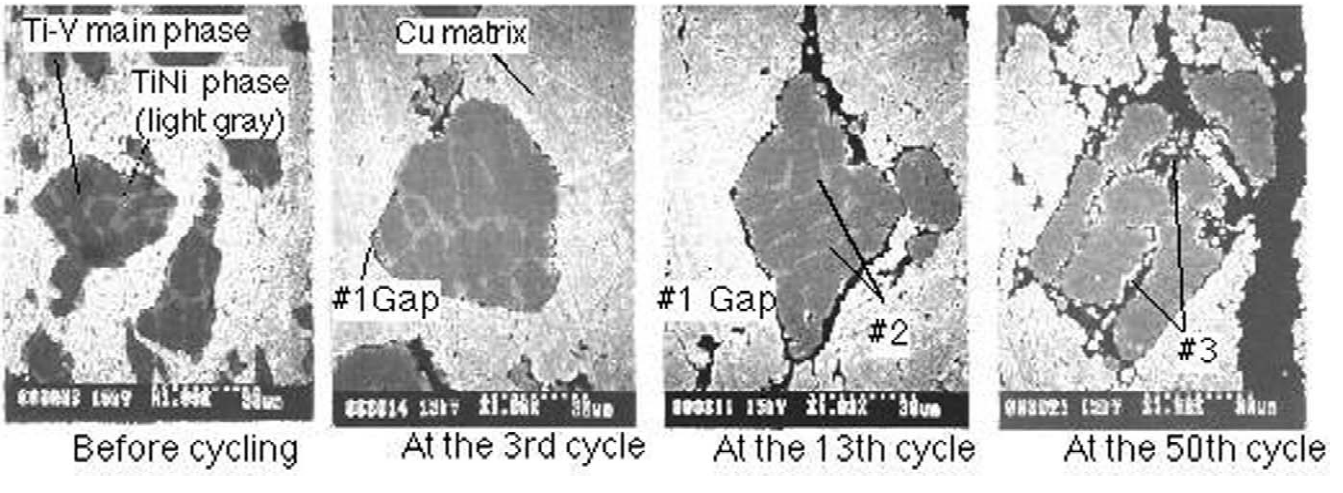

Fig. 3. Cross-sectional views (×1000) of the $V_4TiNi_{0.65}Co_{0.05}Nb_{0.047}Cr_{0.058}$ electrode before cycling and after the third, 13th and 50th cycles. (1) Gaps between an alloy particle and a Cu-powder matrix; (2) a TiNi secondary phase with cracks; (3) a disappeared TiNi secondary phase.

tion and dissolution of the TiNi phase is concluded to be the main origin of deterioration of the electrode of the Ti–V–Ni alloy in dischargeability at higher discharge current density. The Ti–V–Ni alloy is required to improve corrosion resistivity of the TiNi phase in order to apply the alloy to a metal hydride electrode.

References

[1] M. Tsukahara, T. Kamiya, K. Kawasaki, A. Kawabata, S. Sakurai, J. Shi, H.T. Takeshita, N. Kuriyama, T. Sakai, J. Electrochem. Soc. 147 (2000) 2941, and references therein.

[2] N. Kuriyama, T. Sakai, H.T. Takeshita, H. Tanaka, T. Kiyobayashi, N. Takeichi, I. Uehara, J. Alloys Comp. 330–332 (2002) 771.

[3] N. Kuriyama, T. Sakai, H. Miyamura, I. Uehara, H. Ishikawa, T. Iwasaki, J. Alloys Comp. 202 (1993) 183.